

# Photovoltaic Performance of (Al, Mg)-Doped CuCrO<sub>2</sub> for *p*-type Dye-sensitized Solar Cells Application

Ursu Daniel<sup>1,2</sup>, Bănica Radu<sup>1,2</sup>, Vaszilcsin Nicolae<sup>1,\*</sup>

<sup>1</sup>Politehnica University Timisoara, Timisoara, Romania

<sup>2</sup>National Institute for Research and Development in Electrochemistry and Condensed Matter, Timisoara, Romania

**Abstract** Delafossite materials like CuCrO<sub>2</sub> are promising *p*-type semiconductor materials for elaboration of future tandem dye sensitized solar cells. In this paper, we report the successful hydrothermal synthesis of Mg<sup>2+</sup> and Al<sup>3+</sup> doping nanocrystalline CuCrO<sub>2</sub> with very small size and a high surface area of 107 m<sup>2</sup>/g for CuCrO<sub>2</sub>, 110 m<sup>2</sup>/g for CuCr<sub>0.95</sub>Al<sub>0.05</sub>O<sub>2</sub> and 122 m<sup>2</sup>/g for CuCr<sub>0.95</sub>Mg<sub>0.05</sub>O<sub>2</sub>. The specific surface area of our CuCr<sub>0.95</sub>Al<sub>0.05</sub>O<sub>2</sub> and CuCr<sub>0.95</sub>Mg<sub>0.05</sub>O<sub>2</sub> nanocrystalline is the biggest ever reported compared with other materials with delafossite structure used for dye sensitized solar cells (DSSCs) applications. We show that after Al<sup>3+</sup> and Mg<sup>2+</sup> doping, the optical bandgap is shifted with 0.05 eV for Al<sup>3+</sup> doping and 0.27 eV for Mg<sup>2+</sup> doping. From Mott–Schottky plot the acceptor density is N<sub>A</sub>= 1.10 × 10<sup>21</sup> cm<sup>-3</sup> for undoped sample, N<sub>A</sub>= 1.22 × 10<sup>21</sup> cm<sup>-3</sup> for Al<sup>3+</sup> doped and N<sub>A</sub>= 1.56 × 10<sup>21</sup> cm<sup>-3</sup> for Mg<sup>2+</sup> doped. The performance of *p*-type DSSCs based on CuCr<sub>0.95</sub>Al<sub>0.05</sub>O<sub>2</sub> and CuCr<sub>0.95</sub>Mg<sub>0.05</sub>O<sub>2</sub> photocathodes was made using two type of dye: Coumarin C343 and Ruthenium N719. Using Coumarin C343 as dye the short-circuit density (*J*<sub>sc</sub>) is notable increased by approximately 11% for Al<sup>3+</sup> doping and 16% for Mg<sup>2+</sup> doping.

**Keywords** Delafossite, Dye sensitized solar cell, Nanotechnology

## 1. Introduction

One of the challenging problems confronting mankind in the last decade is due to the energy crisis [1]. This is confirmed in according to the International Energy Outlook 2011, where the total world energy consumption will increase with 53% before 2035, driven not only by the economic growth but also by increasing population in developing countries [2]. According to Gr äzel, the energy provided by the sun is approximately 10,000 times more than the global demand (i.e., 3 × 10<sup>24</sup> J/year). Thereby, the sun provides a considerable amount of energy for our planet. If it covering 0.1% of the earth's surface with solar cells that have an efficiency of 10% would fulfill our present needs [3]. Until now the photovoltaic cells are commonly classified as first-, second-, and third- generation devices depending on the underlying technology. First-generation wafer technology is identified by high production costs and has an average efficiency of 20%. Second generation thin film technology offers lower production costs and moderate efficiency (presently 5 ± 10%) [4]. The third generation is dye sensitized solar cells (DSSCs) which present themselves as a very promising photovoltaic technology. They are made of

cheap components that are non-toxic and world-wide available and offer distinctive features such a semi-transparency, multi-color range possibilities, flexibility and light weight applications but also good performance under low light conditions and different solar incident angles [5].

Until now, all the reported regarding at high performance of DSSCs is based on dye-sensitized *n*-type nanocrystalline semiconductors, such as TiO<sub>2</sub>, ZnO, etc. [6], and are known as *n*-DSSCs. The highest efficiency of *n*-DSSCs is 12% by introducing a porphyrin dye with broad light harvesting range [7], and more recently 13% [8]. Therefore, are few studies that are focused on *p*-type semiconductor based DSSCs, and the reported efficiencies were much lower than those of their *n*-type counter parts. According to the literature NiO has been the most frequently reported *p*-type photocathode material in the past [9, 10]. Thereby, major efforts are made to find new nanostructured *p*-DSSCs to favor higher open-circuit voltage (*V*<sub>oc</sub>), short-circuit current (*J*<sub>sc</sub>), and fill factor (*FF*) [11]. In order to improve these parameters, the photocathode for *p*-type DSSC should be required to have some special features: wide band gap, large surface area, high surface chemical affinity, suitable valence band potential and suitably high hole mobility. In addition to these parameters, an important step in the fabrication of DSSCs is to enhance the electron transport and reduce the interfacial charge recombination in photocathodes [12]. Cu (I)-based delafossite compounds, CuMO<sub>2</sub> (M= Al, Ga or Cr)

\* Corresponding author:

vaszilcsin@yahoo.com (Vaszilcsin Nicolae)

Published online at <http://journal.sapub.org/nn>

Copyright © 2016 Scientific & Academic Publishing. All Rights Reserved

are shown very promising performances in *p*-DSSCs because of their intrinsic advantages over NiO such as: high hole conductivity ( $10^{-2}$  -  $10^2$  S cm<sup>-1</sup>), wide band gaps (3.0-3.6 eV) and decent optical transparency (50-80%) [13-18]. One of the disadvantages of the CuCrO<sub>2</sub> compound is a color, compared to CuAlO<sub>2</sub> and CuGaO<sub>2</sub>, which are colorless and have full d-orbitals of M site elements, therefore they are more advantageous for *p*-type DSSCs applications. It is very hard to synthesize nanocrystalline CuAlO<sub>2</sub> or CuGaO<sub>2</sub> with small enough sizes that still remains a great challenge [19]. To increase the efficiency of CuCrO<sub>2</sub> nanocrystals based *p*-DSSCs can choose to decrease particle size which leads to a higher adsorption of dye on their surface, and by increasing the conductivity due to doping to favor the flow of injected charges (and to limit consequently the electron-hole recombination). Up to now the highest photoconversion efficiency for CuCrO<sub>2</sub> is 0.132% if using 4-(Bis-{4-[5-(2,2-dicyano-vinyl)-thiophene-2-yl]-phenyl}-amino)-benzoic acid (P1) dye under optimized conditions [20]. According to the theory of semiconductors the trivalent ion substitution with divalent cations, such as Mg<sup>2+</sup>, Mn<sup>2+</sup>, Ca<sup>2+</sup>, is considered a direct and effective route for improving *p*-type conductivity. Even if the substitution with trivalent cations cannot directly increase the hole concentration, this investigating may provide insight into the complex conduction mechanism in this structure. Until now, only a few studies involving trivalent cation doping have been reported and their use as cathodes in dye sensitized solar cell.

In this work, we report the effect of Mg<sup>2+</sup> and Al<sup>3+</sup> doping nanocrystalline CuCrO<sub>2</sub> with high surface area and we discuss the impact of the photovoltaic performances with two types of dye, Ruthenium-based (N719), and Coumarin C343, using I<sup>-</sup>/I<sub>3</sub><sup>-</sup> dissolved in acetonitrile as redox couple.

## 2. Experimental

### 2.1. Synthesis of CuCr<sub>0.95</sub>Al<sub>0.05</sub>O<sub>2</sub> and CuCr<sub>0.95</sub>Mg<sub>0.05</sub>O<sub>2</sub>

The hydrothermal synthesis procedure of CuCr<sub>0.95</sub>Al<sub>0.05</sub>O<sub>2</sub> and CuCr<sub>0.95</sub>Mg<sub>0.05</sub>O<sub>2</sub> was performed according to our previous work [21], using the following reagents: 1 mmol copper(I) oxide (Cu<sub>2</sub>O, Sigma-Aldrich, 99%), 0.095 mmol chromium (III) hydroxide (Cr(OH)<sub>3</sub>, amorphous was precipitate in aqueous media from Cr(SO<sub>4</sub>)<sub>3</sub> · 12H<sub>2</sub>O in the presence of NaOH, 0.05 mmol aluminum chloride (AlCl<sub>3</sub>, Sigma-Aldrich, 99%) and magnesium oxide (MgO Sigma-Aldrich, 99%) respectively. Sodium hydroxide has been dissolved in 42 mL deionized water to obtain 2.5 M solution, and stirred for 20 min. Temperature was increased to 250 °C for 60 h. The autoclave was cooled down to room temperature naturally. The precipitate was filtered and washed with deionized water and then, the product was dried at 80 °C for 5h.

The structure of products was determined by powder X-ray diffraction (XRD) Panalytical X'pert Pro/PW 3040/60 using Cu-K $\alpha$  radiation with ( $\lambda=1.5418\text{\AA}$ ), in the range  $2\theta =$

10-80°. The morphology of CuCr<sub>0.95</sub>Al<sub>0.05</sub>O<sub>2</sub> and CuCr<sub>0.95</sub>Mg<sub>0.05</sub>O<sub>2</sub> nanocrystals was observed using a transmission electron microscope (TEM, Titan G2 80-200). Brunauer-Emmett-Teller (BET) analysis was used to determine the surface area measurements were achieved by using Quantachrome Nova 1200e device in nitrogen at 77 K temperature. First, all the samples were degassed, in vacuum, at room temperature for 4 hours. The diffuse reflectance spectra (DSR) was obtained using a Lambda 950 UV-Vis-NIR Spectrophotometer with 150 mm integrating sphere in the wavelength range of 300–800 nm. All the measurements were performed at room temperature.

The electrochemical investigations were performed using a Voltalab potentiostat model PGZ 402, with Volta Master 4 (version 7.09) software. A single compartment three-electrode cell was employed along with a platinum wire as counter electrode and the Ag/AgCl/KCl saturate electrode coupled to a Luggin capillary as reference electrode. Thin film of CuCr<sub>0.95</sub>Al<sub>0.05</sub>O<sub>2</sub> and CuCr<sub>0.95</sub>Mg<sub>0.05</sub>O<sub>2</sub> was used as working electrodes (area 0.28 cm<sup>2</sup>). All potentials were referenced to the standard hydrogen electrode (SHE).

The Mott-Schottky (MS) plot was recorded by the electrochemical workstation using the ac impedance method. The principle of this method is to measure the impedance at fixed frequency during a potential. The capacitance of the interface was measured in 0.5M KOH aqueous solutions, in the potential range: 0 ÷ 1 V; with a 20 mV potential step; at fixed frequency: 3 kHz and amplitude of *ac* potential: 20 mV.

### 2.2. Preparation of CuCr<sub>0.95</sub>Al<sub>0.05</sub>O<sub>2</sub> and CuCr<sub>0.95</sub>Mg<sub>0.05</sub>O<sub>2</sub> Films and DSSCs

CuCr<sub>0.95</sub>Al<sub>0.05</sub>O<sub>2</sub> and CuCr<sub>0.95</sub>Mg<sub>0.05</sub>O<sub>2</sub> paste used for film obtaining was made by adding 200  $\mu$ L distilled water, 200  $\mu$ L (1 %) acetic acid in water and 250  $\mu$ L (1%) Triton - 100 polymer in isopropanol as surfactant into about 50 mg of CuCr<sub>0.95</sub>Al<sub>0.05</sub>O<sub>2</sub> and CuCr<sub>0.95</sub>Mg<sub>0.05</sub>O<sub>2</sub> aqueous colloid. This mixture was ultrasonated for 30 minutes in order to disperse the agglomerate particles. After that, the aqueous colloid was heated at 90 °C and mixed with a magnetic stirrer. Resulting paste with suitable viscosity was deposited on FTO-coated glass substrates using Doctor Blade (DB) method. For CuCr<sub>0.95</sub>Al<sub>0.05</sub>O<sub>2</sub> and CuCr<sub>0.95</sub>Mg<sub>0.05</sub>O<sub>2</sub> photocathodes fabrication, FTO coated glass was cleaned using an ultrasonic bath in deionized water, acetone and ethanol, each for 15 min successively. After air drying, the films were sintered under air flow at 350 °C for 1 hour [22] to burn off the organic binder. After cooling to about 100 °C, films were immersed into two type of ethanolic dye solution 0.5 mM Ruthenium N719 dye and 0.5 mM Coumarin C343 dye solution under dark for 48 hour. Catalytic counter electrodes were produced by the thermal decomposition of H<sub>2</sub>PtCl<sub>6</sub> solution on FTO-coated glasses using a hot-wind gun set at 400 °C for 15 minutes. CuCr<sub>0.95</sub>Al<sub>0.05</sub>O<sub>2</sub> and CuCr<sub>0.95</sub>Mg<sub>0.05</sub>O<sub>2</sub> photocathodes were sandwiched together with the platinized

counter electrodes using the electrolyte containing 0.5 M LiI/0.1 M I<sub>2</sub> dissolved in acetonitrile and its were transferred into the cell. Solar cell performances were recorded on a DMM 7352 Series Digital Multimeter, under AM 1.5G simulated sunlight (100 mW/cm<sup>2</sup>).

### 3. Results and Discussions

XRD patterns for CuCr<sub>0.95</sub>Al<sub>0.05</sub>O<sub>2</sub> and CuCr<sub>0.95</sub>Mg<sub>0.05</sub>O<sub>2</sub> nanoproducs prepared by using hydrothermal method are shown in figure 1a. All studied samples have a single rhombohedral (R-3m) delafossite structure. All diffraction peaks are consistent with the standard JCPDF card (No. 00-039-0247) of CuCrO<sub>2</sub>. Impurity phase could not be detected. From XRD patterns using the Scherrer equation can be calculate the average crystal size which indicates that the crystal size decreases with Al<sup>3+</sup> and Mg<sup>2+</sup> doping from 21 nm to 20 nm and 17 nm respectively. The decrease in the crystal size could be assigned to the stabilizing effect of Al<sup>3+</sup> and Mg<sup>2+</sup> on the delafossite crystal structure and the corresponding obstruction of the crystal growth by this resistant impurity [23]. The biggest advantages of CuCrO<sub>2</sub> nanocrystals used in DSSCs applications is the ultra small size which leads to a large amount of adsorbed dye on the semiconductor surface and subsequently to a greater amount of light absorbed. The specific surface area (SSA) of Mg<sup>2+</sup> and Al<sup>3+</sup> doped CuCrO<sub>2</sub>, determined by the Brunauer–Emmett–Teller (BET) method, was found to be 107 m<sup>2</sup>/g for CuCrO<sub>2</sub>, 110 m<sup>2</sup>/g for CuCr<sub>0.95</sub>Al<sub>0.05</sub>O<sub>2</sub> and 122 m<sup>2</sup>/g for CuCr<sub>0.95</sub>Mg<sub>0.05</sub>O<sub>2</sub>. Based on literature data the specific surface area of our CuCr<sub>0.95</sub>Al<sub>0.05</sub>O<sub>2</sub> and CuCr<sub>0.95</sub>Mg<sub>0.05</sub>O<sub>2</sub> nanocrystals is the biggest ever reported compared with other materials with delafossite structure used for DSSCs applications [15, 24]. This high value of

surface area is due to the fact that besides nanoparticles with hexagonal shape that is very well defined, there is also a form of long bars morphology which increases the specific surface. Those morphologies can be seen from the transmission electron microscopy (TEM) images (figure 1 b,c and d) where the nanocrystals with hexagonal shape are around 17-20 nm and their thicknesses are around 5 nm, consistent with XRD, and the bars morphology has a length of 20-40 nm.

Optical bandgaps ( $E_g$ ) of CuCr<sub>0.95</sub>Al<sub>0.05</sub>O<sub>2</sub> and CuCr<sub>0.95</sub>Mg<sub>0.05</sub>O<sub>2</sub> films are calculated from the diffuse reflectance spectra in the wavelength of 300–800 nm, using the  $[(k/s)hv]^2$  vs.  $hv$  plots, (shown in figure 2) where  $hv$  is the photon energy;  $k$  and  $s$  denote the absorption and scattering coefficients respectively. The ratio ( $k/s$ ) can be calculated from the diffuse reflectance spectra using the Kubelka–Munk equation [25, 26]. The direct optical bandgaps of films are 2.88 eV for CuCrO<sub>2</sub>, 2.83 eV for CuCr<sub>0.95</sub>Al<sub>0.05</sub>O<sub>2</sub>, and 2.61 eV for CuCr<sub>0.95</sub>Mg<sub>0.05</sub>O<sub>2</sub>. The decrease of the  $E_g$  with about 0.27 eV for CuCrO<sub>2</sub> doped with Mg<sup>2+</sup>, comparatively with undoped compound, is due to the oxidation to 5% from Cu(I) ions by CuCr<sub>0.95</sub>Mg<sub>0.05</sub>O<sub>2</sub> network for maintaining electroneutrality. It is well known that  $E_g$  amount of CuO is around 1.2 - 1.6 eV, being up to 1 eV lower than the compound Cu<sub>2</sub>O. Until now, according to the literature date improving the open-circuit photovoltage ( $V_{oc}$ ) for compounds CuAlO<sub>2</sub> [19] and CuGaO<sub>2</sub> [14] used in DSSC compared to NiO is strongly influenced by the negative shift of valance band of CuAlO<sub>2</sub> and CuGaO<sub>2</sub> to NiO. For CuCrO<sub>2</sub> the valance band edge position reported in the literature is 5.3 eV [27] while that for NiO is 5.0–5.1 eV [28] below the vacuum level. More negative valance band of semiconductive photocathode corresponds to larger energy gap with respect to the redox potential of the electrolyte, which will result in higher  $V_{oc}$  of  $p$ -type DSC.

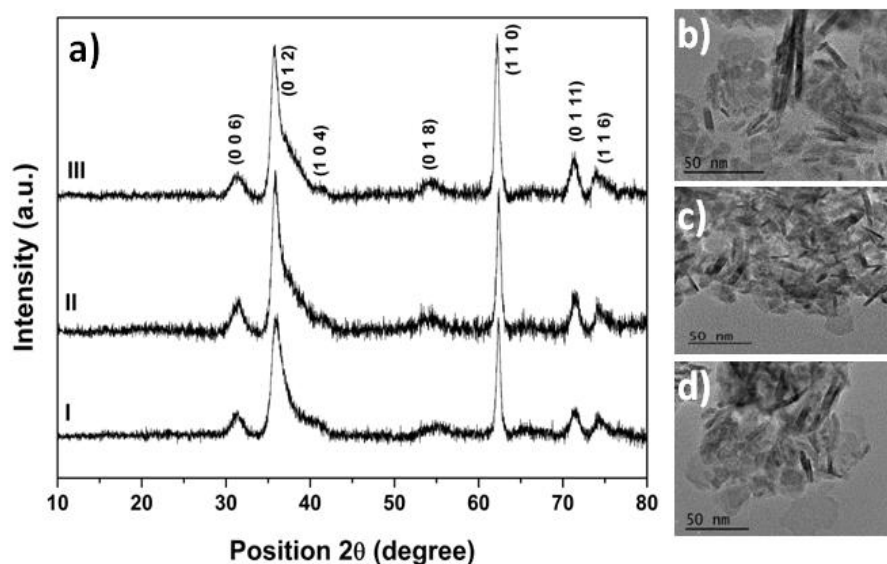


**Figure 1.** a) XRD patterns for I) CuCrO<sub>2</sub>, II) CuCr<sub>0.95</sub>Al<sub>0.05</sub>O<sub>2</sub>, III) CuCr<sub>0.95</sub>Mg<sub>0.05</sub>O<sub>2</sub>, b) TEM image of CuCrO<sub>2</sub>, c) TEM image of CuCr<sub>0.95</sub>Al<sub>0.05</sub>O<sub>2</sub>, d) TEM image of CuCr<sub>0.95</sub>Mg<sub>0.05</sub>O<sub>2</sub>

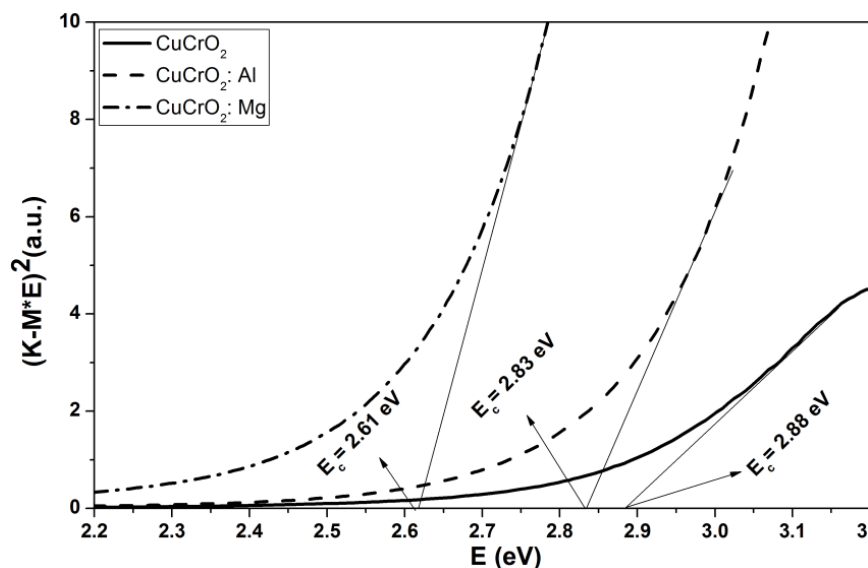


**Figure 2.** Extracted direct optical band gaps of  $\text{CuCrO}_2$ ,  $\text{CuCr}_{0.95}\text{Al}_{0.05}\text{O}_2$ , and  $\text{CuCr}_{0.95}\text{Mg}_{0.05}\text{O}_2$  films

To obtain the flat band potentials and the acceptor concentration of  $\text{CuCr}_{0.95}\text{Al}_{0.05}\text{O}_2$  and  $\text{CuCr}_{0.95}\text{Mg}_{0.05}\text{O}_2$  films, electrochemical impedance measurements were performed using Mott–Schottky measurements. The MS plot (figure 3) of the sample shows a negative slope, which confirms the  $p$ -type semiconducting behavior of  $\text{CuCr}_{0.95}\text{Al}_{0.05}\text{O}_2$  and  $\text{CuCr}_{0.95}\text{Mg}_{0.05}\text{O}_2$  film. The acceptor concentration ( $N_A$ ) and the flat band potential ( $V_{FB}$ ) can be quantified by the Mott-Schottky equation [29]:  $1/C^2 = (2e\epsilon_0\epsilon_N N_A) [(V - V_{FB})kT/e]$ , where  $C$  represents the capacitance of the space charge region,  $\epsilon_0$  - vacuum permittivity,  $\epsilon$  - dielectric constant of  $\text{CuCrO}_2$ ,  $e$  - electron charge,  $V$  - electrode applied potential,  $k$  - Boltzmann constant,  $T$  - absolute temperature and  $N_A$  - acceptor concentration.

For  $\text{CuCrO}_2$  film, the Mott–Schottky plot gives a value for the flat band potential which is 0.55 V vs. SHE, and increase at 0.57V vs. SHE, for  $\text{CuCr}_{0.95}\text{Al}_{0.05}\text{O}_2$ , and  $\text{CuCr}_{0.95}\text{Mg}_{0.05}\text{O}_2$  films. The acceptor density is  $N_A = 1.10 \times 10^{21} \text{ cm}^{-3}$ ,  $N_A = 1.22 \times 10^{21} \text{ cm}^{-3}$  and  $N_A = 1.56 \times 10^{21} \text{ cm}^{-3}$  for  $\text{CuCrO}_2$ ,  $\text{CuCr}_{0.95}\text{Al}_{0.05}\text{O}_2$ , respectively  $\text{CuCr}_{0.95}\text{Mg}_{0.05}\text{O}_2$  films.

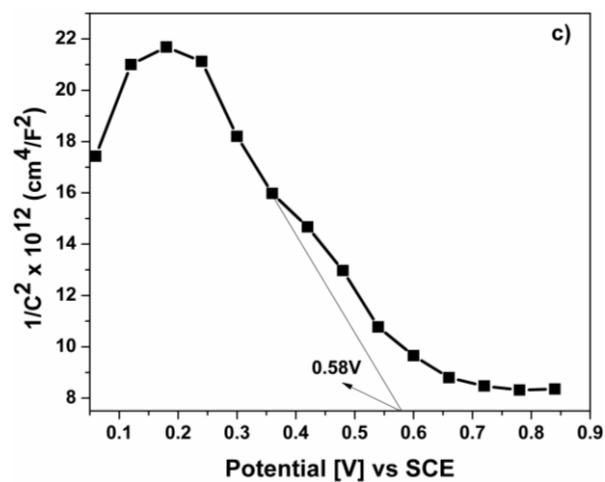
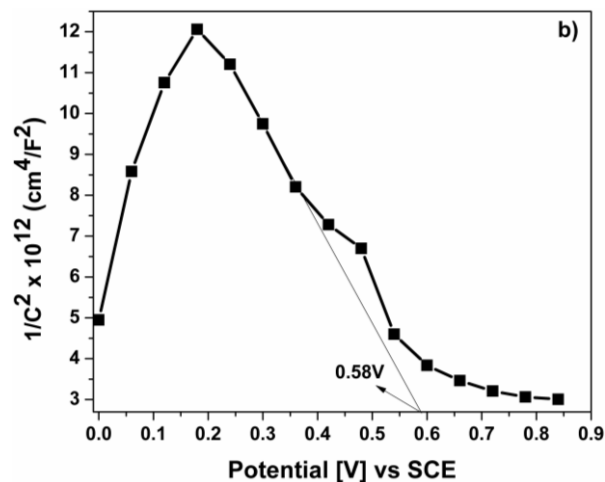
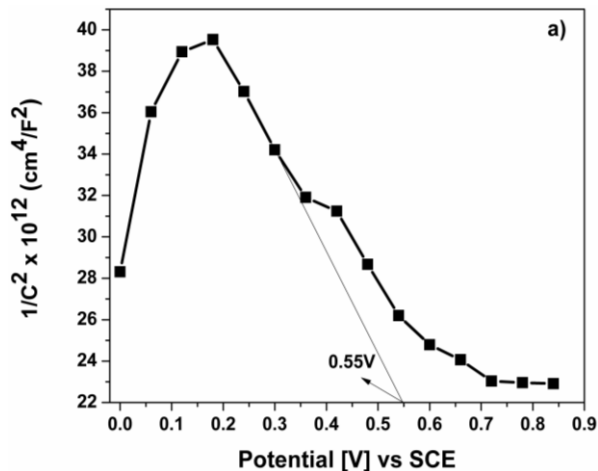


**Figure 3.** Mott–Schottky plot for a)  $\text{CuCrO}_2$ , b)  $\text{CuCr}_{0.95}\text{Al}_{0.05}\text{O}_2$ , c)  $\text{CuCr}_{0.95}\text{Mg}_{0.05}\text{O}_2$

Figure 4 presents the photocurrent-voltage ( $J$ - $V$ ) curve of the  $\text{CuCr}_{0.95}\text{Al}_{0.05}\text{O}_2$ , and  $\text{CuCr}_{0.95}\text{Mg}_{0.05}\text{O}_2$  films based

p-DSSCs under AM 1.5 G illumination. The photocurrent density of DSSCs is determined by the light harvesting efficiency, the hole injection efficiency to the Coumarin C343 and Ruthenium N719 dye molecule binding on the semiconductor surface ( $\text{CuCrO}_2$ ), and the collection efficiency of the hole carriers.

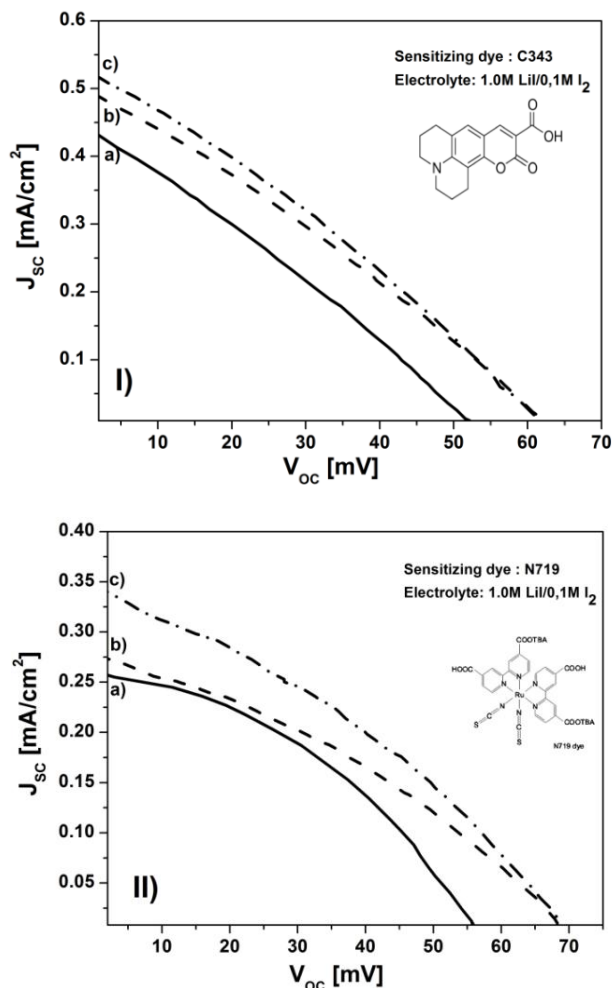


**Figure 4.** Photocurrent-voltage ( $J$ - $V$ ) curve of a)  $\text{CuCrO}_2$ , b)  $\text{CuCr}_{0.95}\text{Al}_{0.05}\text{O}_2$ , c)  $\text{CuCr}_{0.95}\text{Mg}_{0.05}\text{O}_2$  based  $p$ -type DSSCs using I) C343 dye and II) N719 dye (molecular structure show as insert)

The short-circuit density ( $J_{sc}$ ) for  $\text{CuCr}_{0.95}\text{Al}_{0.05}\text{O}_2$ , and  $\text{CuCr}_{0.95}\text{Mg}_{0.05}\text{O}_2$  nanoparticles based electrode, was reported in the range from  $0.44 - 0.52 \text{ mA/cm}^2$  when is using Coumarin C343 as dye and  $0.26 - 0.34 \text{ mA/cm}^2$  when is using Ruthenium N719 as dye. The photovoltage ( $V_{oc}$ ) in  $\text{CuCr}_{1-x}(\text{Al}_x, \text{Mg}_x)\text{O}_2$  ( $x = 0, 0.05$ ) nanoparticles based  $p$ -type DSSCs were found to be  $52 \text{ mV}$ ,  $62 \text{ mV}$  and  $62 \text{ mV}$  for  $\text{CuCrO}_2$ ,  $\text{CuCr}_{0.95}\text{Al}_{0.05}\text{O}_2$ , and  $\text{CuCr}_{0.95}\text{Mg}_{0.05}\text{O}_2$  if using Coumarin C343 as dye and  $56 \text{ mV}$ ,  $68.5 \text{ mV}$  and  $69 \text{ mV}$  for  $\text{CuCrO}_2$ ,  $\text{CuCr}_{0.95}\text{Al}_{0.05}\text{O}_2$ , and  $\text{CuCr}_{0.95}\text{Mg}_{0.05}\text{O}_2$  if Ruthenium N719 is using as dye. The results obtained by us are comparable with the results obtained in the literature taking NiO as reference standard. Although, some materials with delafossite structure such as  $\text{CuGaO}_2$ , where organic dye (P1) it is used, have a higher efficiency ( $V_{oc} = 180 \text{ mV}$ ;  $I_{sc} =$

$0.384 \text{ mA/cm}^2$ ;  $\eta = 0.026\%$ ) [14]. Compared to the materials obtained by us where we use as dye C343, the  $I_{sc}$  is stil low. This increase of  $I_{sc}$  to 29% for  $\text{CuCr}_{0.95}\text{Mg}_{0.05}\text{O}_2$  compared with  $\text{CuGaO}_2$  is due to the small width of the particles resulting in a high specific surface area, thus can absorb a greater amount of dye on the nanoporous film.

## 4. Conclusions

In conclusion, we report the hydrothermally synthesis effect of  $\text{CuCrO}_2$  doped with  $\text{Al}^{3+}$  and  $\text{Mg}^{2+}$  with ultrasmall nanocrystals, having high surface area, the highest ever reported for materials with delafossite structure used in DSSCs. The nanosized particles play a crucial role in the enhancement of cathodic current efficiency. Their applications as photocathodes were first demonstrated, using two type of dye: Coumarin C343 and Ruthenium N719, and  $\text{I}^-/\text{I}_3^-$  as redox couple thus being obtained yield conversion efficiencies similar to those commonly reported for NiO. In the case of used Coumarin C343 as dye, the short-circuit density ( $J_{sc}$ ) is notable increased from  $0.44 \text{ mA/cm}^2$  for undoped sample to  $0.52 \text{ mA/cm}^2$  for  $\text{CuCr}_{0.95}\text{Mg}_{0.05}\text{O}_2$ . This increase of  $I_{sc}$  with 29% for  $\text{CuCr}_{0.95}\text{Mg}_{0.05}\text{O}_2$ , compared with  $\text{CuGaO}_2$  [16], is due to the small width of the particle resulting in a high specific surface area.

In future investigations, our attention will be focused to further optimize the dye and the redox mediators, to improve the photovoltaic performances of the  $p$ -type DSSCs. In addition, we try to increase the  $V_{oc}$  using the “surface passivation” with different materials.

## ACKNOWLEDGEMENTS

This paper is partial supported by the Sectoral Operational Programme Human Resources Development (SOP HRD), financed from the European Social Fund and by the Romanian Government under the projects numbers POSDRU/159/1.5/S/134378 and POSDRU/159/1.5/S/137070 and by a grant of the Romanian Ministry of National Education, CNCS – UEFISCDI, project number PN-II-ID-PCE-2012-4-0398.

## REFERENCES

- [1] N. Dematage, E.V.A. Premalal, A. Konno, “Employment of CuI on  $\text{Sb}_2\text{S}_3$  Extremely Thin Absorber Solar Cell: N719 Molecules as a Dual Role of a Recombination Blocking Agent and an Efficient Hole Shuttle” *Int. J. Electrochem. Sci.*, 9, pp. 1729 – 1737, 2014.
- [2] J Conti, PH., *International Energy Outlook 2011*. U.S. Energy Administration, (2011).
- [3] M. Gratzel, *Nature*, “Photoelectrochemical cells” vol. 414, pp. 338-344, 2001.

- [4] M. Kouhnavard, S. Ikeda, N.A. Ludin, N.B. Ahmad Khairudin, B.V. Ghaffari, M.A. Mat-Teridi, M.A. Ibrahim, S. Sepeai, K. Sopian, "A review of semiconductor materials as sensitizers for quantum dot-sensitized solar cells" *Renewable and Sustainable Energy Reviews* vol. 37, pp.397–407, 2014.
- [5] L.M. Goncalves, V.Z. Bermudez, H.A. Ribeiro, A.M. Mendes, "Dye-sensitized solar cells: A safe bet for the future", *Energy and Environmental Science* vol.1 pp. 655-667, 2008
- [6] N. Memarian, I. Concina, A. Braga, S.M. Rozati, A. Vomiero, G. Sberveglieri, "Hierarchically Assembled ZnO Nanocrystallites for High-Efficiency Dye-Sensitized Solar Cells" *Angew. Chem. Int. Ed. Vol. 50*, pp. 12321–12325, 2011.
- [7] A. Yella, H.W. Lee, H.N. Tsao, C. Yi, A.K. Chandiran, M. K. Nazeeruddin, E.W.G. Diau, C.Y. Yeh, S.M. Zakeeruddin and M. Grätzel, "Porphyrin-Sensitized Solar Cells with Cobalt (II/III)-Based Redox Electrolyte Exceed 12 Percent Efficiency" *Science* vol. 334, pp. 629-634, 2011.
- [8] S. Mathew, A. Yella, P. Gao, R. Humphry-Baker, B. Curchod, N. Ashari-Astani, I. Tavernelli, U. Rothlisberger, Md. K. Nazeeruddin and M. Grätzel, "Dye-sensitized solar cells with 13% efficiency achieved through the molecular engineering of porphyrin sensitizers", *Nature Chemistry*, vol. 6, pp. 242–247, 2014.
- [9] S. Mori, S. Fukuda, S. Sumikura, Y. Takeda, Y. Tamaki, E. Suzuki and T. Abe, *J. Phys. Chem.* "Charge-Transfer Processes in Dye-Sensitized NiO Solar Cells" Vol. C 112 pp. 16134-16139, 2008.
- [10] Y. Mizoguchi and S. Fujihara, *Electrochem*, "Fabrication and Dye-Sensitized Solar Cell Performance of Nanostructured NiO/Coumarin 343 Photocathodes" *Solid-State Lett.*, vol. 11, p. K78–K80, 2008.
- [11] Z. Huang, G. Natu, Z. Ji, M. He, M. Yu, Y. Wu, "Probing the Low Fill Factor of NiO p-Type Dye-Sensitized Solar Cells", *J. Phys. Chem. Vol. C 116*, pp. 26239–26246, 2012.
- [12] V. Mani, S.M. Chen, B.S. Lou, "Three Dimensional Graphene Oxide-Carbon Nanotubes and Graphene - Carbon Nanotubes Hybrids", *Int. J. Electrochem. Sci.*, vol.8, pp.11641-11660, 2013.
- [13] J. Ahmed, C. K. Blakely, J. Prakash, S. R. Bruno, M. Yu, Y. Wu, V. V. Poltavets, "Scalable synthesis of delafossite CuAlO<sub>2</sub> nanoparticles for p-type dye-sensitized solar cells applications" *Journal of Alloys and Compounds*, vol. 591, pp. 275–279, 2014.
- [14] M. Yu, G. Natu, Z. Ji, and Y. Wu, "p-Type Dye-Sensitized Solar Cells Based on Delafossite CuGaO<sub>2</sub> Nanoplates with Saturation Photovoltages Exceeding 460 mV" *J. Phys. Chem. Lett. Vol. 3* pp. 1074–1078, 2012.
- [15] D. Xiong, Z. Xu, X. Zeng, W. Zhang, W. Chen, X. Xu, M. Wanga and Y.B. Cheng, "Hydrothermal synthesis of ultrasmall CuCrO<sub>2</sub> nanocrystal alternatives to NiO nanoparticles in efficient p-type dye-sensitized solar cells" *J. Mater. Chem. Vol. 22*, pp. 24760– 24768, 2012.
- [16] Z. Xu, D. Xiong, H. Wang, W. Zhang, X. Zeng, L. Ming, W. Chen, X. Xu, J. Cui, M. Wang, S. Powar, U. Bach, Y.B. Cheng, "Remarkable photocurrent of p-type dye-sensitized solar cell achieved by size controlled CuGaO<sub>2</sub> nanoplates" *J. Mater. Chem. A*, vol. 2 pp. 2968-297, 2014.
- [17] D. Ursu, M. Miclau, R. Banica, N. Vaszilcsin, "Impact of Fe doping on performances of CuGaO<sub>2</sub> p-type dye-sensitized solar cells" *Materials Letters* vol.143 pp. 91–93, 2014
- [18] D. H. Ursu, M. Miclău, R. Bănică and I. Grozescu, "Hydrothermal synthesis and optical characterization of Ni-doped CuCrO<sub>2</sub> nanocrystals", *Phys. Scr.*, pp. 014053-014053, 2013.
- [19] A. Nattestad, X.L. Zhang, U. Bach, Y.B. Cheng, "Dye-sensitized CuAlO<sub>2</sub> photocathodes for tandem solar cell applications" *J. Photonics Energy* vol. 1 011103-011111, 2011.
- [20] D. Xiong, W. Zhang, X. Zeng, Z. Xu, W. Chen, J. Cui, M. Wang, L. Sun, Y.B. Cheng, "Enhanced Performance of p-Type Dye-Sensitized Solar Cells Based on Ultrasmall Mg-Doped CuCrO<sub>2</sub> Nanocrystals" *ChemSusChem. Vol.8* pp. 1432 - 1437, 2013.
- [21] M. Miclau, D. Ursu, S. Kumar, I. Grozescu, "Hexagonal polytype of CuCrO<sub>2</sub> nanocrystals obtained by hydrothermal method" *Journal of Nanoparticle Research*, 14 (2012) 1-8
- [22] D. Ursu, M. Miclau, "Thermal stability of nanocrystalline 3R-CuCrO<sub>2</sub>" *Journal of Nanoparticle Research* vol. 16, pp. 2160 - 2167, 2013
- [23] R. Bywalez, S. Götzendörfer, P. Löbmann, "Structural and physical effects of Mg-doping on p-type CuCrO<sub>2</sub> and CuAl<sub>0.5</sub>Cr<sub>0.5</sub>O<sub>2</sub> thin films" *J. Mater. Chem* vol. 20, 6562 - 6570, 2010.
- [24] A. Renaud, L. Cario, P. Deniard, E. Gautron, X. Rocquefelte, Y. Pellegrin, E. Blart, F. Odobel, and S. Jobic, "Impact of Mg Doping on Performances of CuGaO<sub>2</sub> Based p-Type Dye-Sensitized Solar Cells" *J. Phys. Chem. Vol. C 118* pp. 54–59, 2014.
- [25] P. Kubelka, F. Munk, "An article on optics of paint layers" *Zh. Tekh. Fiz. Vol.12*, pp. 593-620, 1931
- [26] P. Kubelka, "New contributions to the optics of intensely light-scattering materials" *J. Opt. Soc. Am. Vol. 38* pp. 448-457, 1948
- [27] F.A. Benko and F.P. Koffyberg, "Preparation and opto-electronic properties of semiconducting CuCrO<sub>2</sub>" *Mater. Res. Bull.*, vol.6, pp. 753-757, 1986.
- [28] A. Nattestad, M. Ferguson, R. Kerr, Y.B. Cheng and U. Bach, "Dye-sensitized nickel(II) oxide photocathodes for tandem solar cell applications." *Nanotechnology* vol. 19, pp. 295304 - 295304, 2008.
- [29] L.C. Wang, M. Tao, "Fabrication and characterization of p-n homojunctions in cuprous oxide by electrochemical deposition," *Electrochem. Solid State Lett.*, vol. 10 . pp. H248-H250, 2007.